Proceedings of the 18th World Congress
The International Federation of Automatic Control
Milano (Italy) August 28 - September 2, 2011

Design of Dynamic Experiments Versus Model-Based Optimization of Batch Crystallization Processes

Andrew Fiordalis and Christos Georgakis [1]

Department of Chemical and Biological Engineering
and Systems Research Institute
Tufts University
Medford, MA 02155 USA

Abstract: A new data-driven optimization methodology is applied to a batch cooling crystallization simulation to evaluate how it compares with a model-based optimization technique. The method, Design of Dynamic Experiments [Georgakis, 2009], is an extension of the classical Design of Experiments approach and can be applied to any process where time-variant profiles are important for optimizing key objectives of the process. As a data-driven approach with no first-principles model required for process optimization, this methodology may be particularly useful for complex processes for which no knowledge-driven model exists or where the objective function cannot be modeled.

Keywords: Optimization; Design of Experiments; Batch Crystallization.

1. INTRODUCTION

Batch crystallization is an important industrial unit operation commonly found in the pharmaceutical and specialty/fine chemical industries where high-value products are produced in small batches. Process optimization is imperative for these high-value products in order to produce crystals with desirable properties, maximize yield, and minimize lot-to-lot variability. Current optimization methodologies typically require the use of a first-principles model. Model-based techniques work well, but models describing complex pharmaceutical crystallizations for systems exhibiting polymorphs, localized concentration and temperature gradients, or crystals with multiple internal coordinates do not generally exist. Data-driven techniques based on the Design of Experiment (DoE) methodology can also be used to generate response surface models which can be used for process optimization. The major drawback of this approach is its inability to evaluate time-variant factors, such as temperature, antisolvent addition, or supersaturation trajectories, that are typically important in batch crystallization processes.

Simple, one-dimensional crystallization models that neglect crystal agglomeration and breakage are common in the literature [Worlitschek and Mazzotti, 2004, Xie et al., 2001, Ward et al., 2006, Nagy et al., 2008] and provide insight into the inner workings of crystallization processes in terms of growth and nucleation kinetics. These models allow for the calculation of crystal size distribution outcomes and are often used in process optimization routines to determine an optimum trajectory (temperature, antisolvent, supersaturation) that will result in a predefined crystal size distribution [Worlitschek and Mazzotti, 2004, Nagy et al., 2008, Hu et al., 2005, Choong and Smith, 2004, Sarkar et al., 2006, Lang et al., 1999]. However, first-principle models for more complex crystallization systems (polymorphic crystallization systems, antisolvent systems with localized temperature and concentration gradients, etc.) are more difficult to develop and rarely found in the literature.

In many cases, the time and effort required to develop a comprehensive knowledge-driven crystallization model is too costly and this cost will not be offset by the value added to the process through the development of such a first-principles model. Furthermore, important optimization objectives such as purity, product stability, or downstream filterability are difficult to model or cannot be modeled. In such cases, optimizing a certain aspect of the final crystal size distribution (CSD) based on a first-principles model may not satisfy one of these more data-oriented optimization objectives.

Optimization of the cooling profile for batch crystallizers is a well-studied research topic. In order to optimize the temperature trajectory, an objective function in terms of the final crystal characteristics at the end of the batch must be specified. Examples of optimization objectives include maximizing crystal growth, minimizing nucleation, achieving a target CSD, or maximizing or minimizing some characteristic of the final crystal distribution. Two methods for constructing the temperature profile to be optimized in a model-based dynamic optimization problem include discretization [Ward et al., 2006, Lang et al., 1999] and parameterization [Choong and Smith, 2004]. In such cases, determination of the optimum cooling trajectory requires a first-principles crystallization model. The optimum temperature profile is found using a constrained, non-linear optimization routine which maximizes or mini-

[1] Corresponding Author: *christos.georgakis@tufts.edu*

mizes the objective function subject to the crystallization model and any system constraints.

Many researchers have determined optimum temperature profiles for a number of different crystallization models using various objective functions. Choong and Smith [2004] evaluated the batch cooling crystallization of citric acid in water. Worlitschek and Mazzotti [2004] studied a batch cooling crystallization of paracetamol in ethanol. Hu et al. [2005] and Sarkar et al. [2006] looked at the batch cooling crystallization of potassium sulfate in water. Ward et al. [2006] and Chung et al. [1999] evaluated a batch cooling crystallization of potassium nitrate in water.

In each of these papers, relatively simple crystallization models are used in the optimization algorithm. Each model consists of a one-dimensional population balance equation (PBE) coupled with a mass balance equation. Similar assumptions are made in each model: 1) size-independent growth; 2) no crystal agglomeration or breakage; 3) a nucleation rate equal to either the sum of the primary and secondary nucleation rates or based solely on the secondary nucleation rate, and; 4) a perfectly mixed crystallizer with crystals homogeneously distributed and no temperature or concentration gradients.

In this paper we evaluate a new data-driven optimization technique developed by Georgakis [2009] called Design of Dynamic Experiments (DoDE). This new data-driven methodology is an extension of the classical Design of Experiments (DoE) technique [Montgomery, 2005] and allows for the systematic evaluation of time-variant input profiles for batch process optimization without the need for a first-principles process model. The DoDE methodology is, therefore, beneficial for processes where a first-principles model does not exist or is too costly to develop. In this work, we show how the DoDE approach is used to optimize the cooling trajectory for a batch crystallization and compare these results with those obtained using a well established model-based optimization technique. Here, we document that, for the present case where a model is at hand, the DoDE approached provides an optimum that is very comparable to the model-based one. This builds support that the DoDE methodology can achieve a very respectable optimization result for crystallization processes without a knowledge-driven model.

2. CRYSTALLIZATION MODEL AND OPTIMIZATION OBJECTIVES

The seeded, potassium nitrate (KNO_3) batch crystallization model evaluated by Ward et al. [2006] and Chung et al. [1999] was used to compare the DoDE optimization methodology to a well established model-based optimization technique. The method of moments [Hulburt and Katz, 1964] was utilized to solve the crystallization model in terms of the moments of the total crystal size distribution. The model parameters and initial seed conditions listed in the paper by Ward et al. [2006] were used in the simulation. The total batch time (t_b) was taken as 160 minutes. The initial crystallizer temperature, T_i, was taken as 32°C and the final temperature, T_f, was 22°C. The cooling rate was constrained as $-0.1^{\circ}\text{C/min} \leq \frac{\mathrm{d}T}{\mathrm{d}t} \leq 0^{\circ}\text{C/min}$. The initial relative supersaturation value was taken as 2.8×10^{-3}.

Ward et al. [2006] grouped the optimization results found by past researchers who evaluated objective functions based on the moments of the final crystal size distribution into early and late growth policies. Based on their results, two optimization objectives were selected in order to compare the flexibility of the DoDE optimization technique to the model-based optimization technique. The first objective resulted in an early growth policy (concave to linear cooling trajectory) and the second objective resulted in a late growth policy (convex cooling trajectory).

The first objective selected, *minimize* m_0, results in an early growth policy. This objective minimizes the total number of new crystals formed during the crystallization. In terms of the moments of the CSD we wish to minimize the zeroth moment (m_0).

The second objective selected, *maximize* m_4/m_3, results in a late growth policy. Here, we wish to maximize the mass average length of the crystals. In terms of the moments of the CSD we wish to maximize the ratio of the forth moment to the third moment. This objective was found to be insensitive to small crystals [Chung et al., 1999] but was selected because, in terms of the moments of the total crystal size distribution, it results in a late growth policy for the crystallization.

For both objectives, the optimization is subject to the KNO_3 crystallization model and the constraints listed above.

3. DESIGN OF DYNAMIC EXPERIMENTS

The Design of Dynamic Experiments methodology developed by Georgakis [2009] is an extension of the classical Design of Experiments technique. DoDE allows an experimentalist to look at time-variant input profiles in a systematic way by evaluating dynamic subfactors using design and analysis tools developed for DoE. The classical DoE approach develops a set of experiments based on the number of factors (variables) being evaluated, the number of levels (operating values) each factor can assume, and the type of experimental design. The factors evaluated in a DoE design are time-invariant, meaning the factor remains constant over the course of an experiment. The time-invariant nature of the classical DoE method is a major limitation when designing experiments for systems where a dynamic input profile is preferred, such as the cooling profile for a batch crystallization.

Like the optimization technique mentioned earlier by Choong and Smith [2004] the Design of Dynamic Experiments method utilizes a parameterized input profile. However, unlike the model based approach, DoDE is entirely data-driven and requires no first-principles model in order to optimize the process. This means that optimum, time-variant input profiles for complex batch processes can be calculated for systems where no first-principles model exists. The optimization is carried out after all experiments are performed using response surface modeling techniques developed for the classical Design of Experiments methodology [Montgomery, 2005].

The parameterized input profiles are written as a series expansion in terms of orthogonal basis functions. Each basis function is multiplied by a dynamic subfactor (pa-

rameter) that is used to adjust the shape of the profile. The dynamic subfactors are taken as variables in the experimental design and allow for the systematic evaluation of the dynamic input profiles on the response variable quantifying the process objective.

For this study, the cooling rate profile was parameterized as an expansion of the shifted Legendre polynomials. The shifted Legendre polynomials were selected as they represent a complete set of orthogonal functions on the domain $[0, 1]$. This allows for evaluation of the time-variant cooling rate profiles over the dimensionless time span $[0, 1]$. The dimensionless time is defined as $\tau = t/t_b$, where t_b is the batch time. The general expansion for the dimensionless cooling rate equation is

$$\frac{\mathrm{d}\theta}{\mathrm{d}\tau} = -P_0(\tau) - \sum_{i=1}^{n} a_i P_i(\tau). \tag{1}$$

$P_0(\tau)$ and $P_i(\tau)$ are the zeroth and i^{th} shifted Legendre polynomials, respectively. a_i is the i^{th} dynamic subfactor (DSF).

In the case of two dynamic subfactors ($n = 2$), the dimensionless cooling rate is parameterized as

$$\frac{\mathrm{d}\theta}{\mathrm{d}\tau} = -1 - a_1(2\tau - 1) - a_2(1 - 6\tau + 6\tau^2). \tag{2}$$

θ is dimensionless temperature ($\theta = \frac{T - T_i}{T_i - T_f}$). The leading value of -1 in (2) forces the temperature profile at $t = 0$ and $t = t_b$ to take the values T_i and T_f, respectively.

The dimensionless temperature profile is determined by integrating (2), which leads to

$$\theta(\tau) = -\tau - a_1(\tau^2 - \tau) - a_2(\tau - 3\tau^2 + 2\tau^3). \tag{3}$$

The design space for the dynamic subfactors is determined by enforcing the cooling rate constraints on the cooling rate profile. In dimensionless form the constraint is

$$-1.6 \leq \frac{\mathrm{d}\theta}{\mathrm{d}\tau} \leq 0. \tag{4}$$

The design space is represented as the intersection of the following inequalities

$$-1.6 \leq \frac{\mathrm{d}\theta(0)}{\mathrm{d}\tau} \leq 0 \tag{5}$$

$$-1.6 \leq \frac{\mathrm{d}\theta(1)}{\mathrm{d}\tau} \leq 0 \tag{6}$$

$$-1.6 \leq \frac{\mathrm{d}\theta(\tau^*)}{\mathrm{d}\tau} \leq 0 \tag{7}$$

where τ^* is found by solving (8) for τ.

$$\frac{\mathrm{d}}{\mathrm{d}\tau}\left(\frac{\mathrm{d}\theta}{\mathrm{d}\tau}\right) = 0 \tag{8}$$

Equations (5) and (6) limit the value of the cooling rate at $t = 0$ and $t = t_b$, respectively. Equation (7) restrict the maximum and minimum value of the cooling rate for $0 < t < t_b$.

Evaluation of (5)-(7) leads to the following four inequalities, which describe the design space in terms of the two dynamic subfactors.

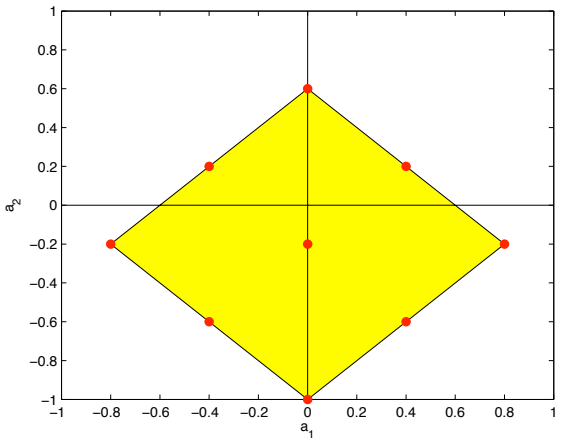

Fig. 1. Design space for two dynamic subfactors. Experimental points for a full factorial design are shown in red.

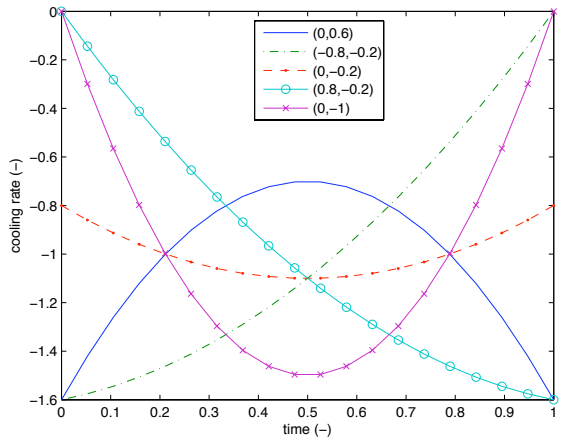

Fig. 2. Cooling rate profiles generated using five of the nine design points from within the design space shown in Fig. 1.

$$-a_1 + a_2 \leq 0.6 \tag{9}$$

$$a_1 + a_2 \leq 0.6 \tag{10}$$

$$a_1 - a_2 \leq 1 \tag{11}$$

$$-a_1 - a_2 \leq 1 \tag{12}$$

The intersection of (9)-(12) is represented by the shaded diamond in Fig. 1. The solid circles in Fig. 1 represent experimental design points equivalent to a two-factor, three-level full factorial design or a central composite design (CCD) where the corner points are located at the midpoints of the edges and the axial points are located at the corners of the diamond. Figures 2 and 3 depict the dimensionless cooling rate and temperature trajectories, respectively, for five of the nine experimental design points. Note that all cooling rates satisfy (4) and all temperature trajectories generated from points inside the design space are bound from above and below by the cooling profiles generated at the $(0.8, -0.2)$ and $(-0.8, -0.2)$ design points, respectively.

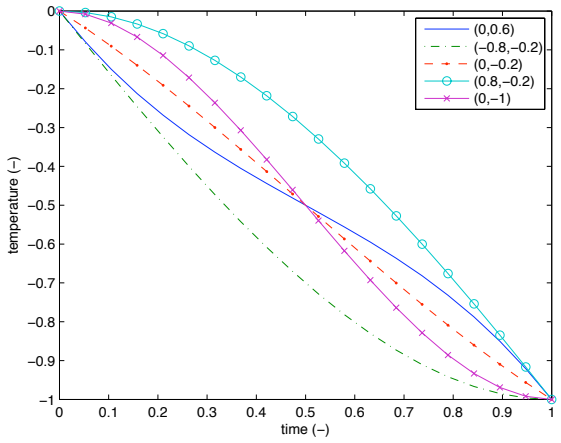

Fig. 3. Temperature profiles generated using five of the nine design points from within the design space shown in Fig. 1. These cooling trajectories correspond to the cooling rate profiles shown in Fig. 2.

4. RESULTS

We now apply the DoDE to optimize the cooling trajectory for a seeded, potassium nitrate batch crystallization simulation and compare the optimization results with those obtained from a model-based optimization technique.

4.1 Model Based Optimization

The collocation on finite elements method presented by Lang and Biegler [2007] was used to solve the model-based optimization problem. This method transforms a system of differential equations into a system of algebraic equations. For the potassium nitrate crystallization model the differential moment equations along with the mass balance equation were converted into a system of algebraic equations representing the state variables of the crystallization system. Each of these state variables was then evaluated at each of the collocation points. The optimization routine calculates a value for the objective function based on the values of the discretized input profile, in this case the cooling trajectory, at each collocation point and adjusts the values of the input profile, subject to the model constraints, until an optimum value for the objective is found.

We solved the model-based optimization problem for the potassium nitrate crystallization system using the General Algebraic Modeling System (GAMS) [http://www.gams.com] and the nonlinear, constrained optimization solver, SNOPT [http://www.sbsi-sol-optimize.com/asp/sol_product_snopt.htm], on the NEOS Server for Optimization [http://www-neos.mcs.anl.gov].

For the first objective, minimize m_0, the optimum value was found to be 2.61×10^6 #crystals/kg. The resulting optimum cooling profile is shown in Fig. 4. For the second objective, maximize m_4/m_3, the optimum value was found to be 5.97×10^{-4} m. The resulting optimum cooling profile is shown in Fig. 5. In order to ensure a global optimum was found, the optimization routine was run using a number of different initial cooling profiles. In all cases they converged to the results reported.

4.2 Design of Dynamic Experiments Optimization

The experimental data required to implement the DoDE optimization strategy was simulated using the potassium nitrate crystallization model discussed in Section 2. In order to introduce variability into the simulated results a normally-distributed random error not greater than 2%, N(0,0.02/3), was multiplicatively added to the response variables, m_0 and m_4/m_3, at the end of each simulated experiment.

Two Dynamic Subfactors In order to determine the optimum values of the dynamic subfactors, a_1 and a_2, in the parameterized cooling rate function (2), data was simulated at each of the experimental points shown in Fig. 1. In addition to these nine data points, three additional center point experiments were simulated. The replicated center point experiments were used to estimate a model-independent variance value at the center of the design space, which was used to calculate the Lack of Fit (LoF) statistic. The lack of fit statistic is used to evaluate whether the form of the response surface model (RSM) adequately fits the experimental data.

Second-order response surface models were fit to the simulated response variables, m_0 and m_4/m_3. Before estimating the model parameters, the dynamic subfactors, a_1 and a_2, were scaled to range between -1 and $+1$ using the following variable substitutions:

$$\bar{a}_1 = \frac{a_1}{0.8} \tag{13}$$

$$\bar{a}_2 = \frac{a_2 + 0.2}{0.8}. \tag{14}$$

This scaling was performed so the magnitude of the significant parameter estimates were of the same order and so each estimate was made with similar precision [Montgomery, 2005].

A second-order response surface model is defined by

$$\hat{y} = \hat{\beta}_0 + \sum_i \hat{\beta}_i \bar{a}_i + \sum_i \sum_j \hat{\beta}_{ij} \bar{a}_i \bar{a}_j + \sum_i \hat{\beta}_{ii} \bar{a}_i^2 \qquad i = 1, 2, \ldots \quad j = 2, 3, \ldots \quad i < j. \tag{15}$$

$\hat{y}$ is the predicted response variable or objective function, in this case m_0 or m_4/m_3. $\hat{\beta}_i$ are the parameter estimates and $\bar{a}_i$ are the scaled dynamic subfactors (DoDE) or static factors (DoE).

Second-order response surface models were fit to the data for each response variable using linear least squares regression. Models and parameter estimates were tested at a significance level of $\alpha = 0.05$ along with all other statistical tests. This means any statistic with a $p - value \leq 0.05$ is significant, leading to rejection of the null hypothesis for the test in question. The parameter estimates and 95% confidence intervals for the m_0 and m_4/m_3 response surface models are listed in Table 1. Parameters with values of zero were found to be nonsignificant (i.e. the null hypothesis, $\beta_i = 0$, was not rejected). The significance of the parameter estimates was evaluated using a partial t-test.

The following steps were taken to test the validity of each response surface model: 1) the variance inflation factors

Table 1. RSM Parameter Estimates and 95% Confidence Intervals with VIF

	Response m_0 ($\times 10^{-5}$)	m_0 VIF	Response m_4/m_3 ($\times 10^5$)	m_4/m_3 VIF
$\hat{\beta}_0$	26.50 ± 0.16	-	55.39 ± 0.22	-
$\hat{\beta}_1$	0	-	2.51 ± 0.35	1
$\hat{\beta}_2$	-0.90 ± 0.19	1	-1.44 ± 0.35	1
$\hat{\beta}_{12}$	0	-	1.85 ± 1.22	1
$\hat{\beta}_{11}$	1.49 ± 0.30	1.13	0	-
$\hat{\beta}_{22}$	0.71 ± 0.30	1.13	-0.62 ± 0.50	1

(VIF) were evaluated to determine if multicollinearity existed between regressors; 2) the model residuals were determined to ensure they were normally distributed; 3) the $R^2(adj)$ and $R^2(pred)$ values were calculated to determine how much of the variability in the data was explained by the RSM, and; 4) the lack of fit statistic was calculated for each RSM to ensure the model adequately fit the data.

The VIF values reported in Table 1 are a measure of the amount of multicollinearity between regressors, in this case the dynamic subfactors, in the model. A value of one indicates no multicollinearity, while values above $\approx 5-10$ indicate the presence of multicollinearity between two or more of the regressors [Myers and Montgomery, 1995]. Multicollinearity leads to parameters estimates with large standard errors and models with poor predictive capabilities. The VIF values for the two RSM models have values of one or close to one indicating the regressors are not correlated.

An evaluation of the model residuals (data not presented) found them to be structureless and normally distributed. No patterns in the data were seen when the residuals were plotted versus the predicted response or against experiment number. The Shapiro-Wilk W test was used to test that the model residuals were distributed normally for each response. In both cases the test statistic had a $p-value > 0.05$ indicating that the null hypothesis, the residuals are normally distributed, could not be rejected.

$R^2(adj)$ and $R^2(pred)$ values for each RSM model are listed in Table 2. The $R^2(adj)$ value describes how much of the variability in the response data is accounted for by the model. It is similar to the R^2 statistic but is corrected based on the number of factors in the model, making it a better indication of how the variability in the data is accounted for. In the case of the m_0 and m_4/m_3 RSM, we see that 96% and 97% of the variability in the data is accounted for by each model, respectively.

The $R^2(pred)$ value is an indication of how much of the variability in the predicted response is accounted for by the RSM. Values close to 100% are desired. The $R^2(pred)$ values for the m_0 and m_4/m_3 RSM's indicate that the models will account for 88% and 95% of the variability, respectively, when using the model to predict outcomes within the design space.

The lack of fit statistic is calculated by splitting the sum of the square of the errors for the RSM into a pure error and lack of fit component. The pure error is calculated using the replicated center point experiments, four in this work, making it independent of the model error. The lack of fit error is calculated using the model residuals. If the ratio of

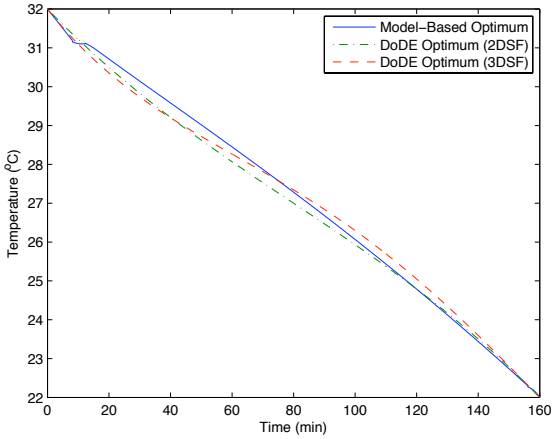

Fig. 4. Optimum temperature profiles for the optimization objective, *minimize* m_0.

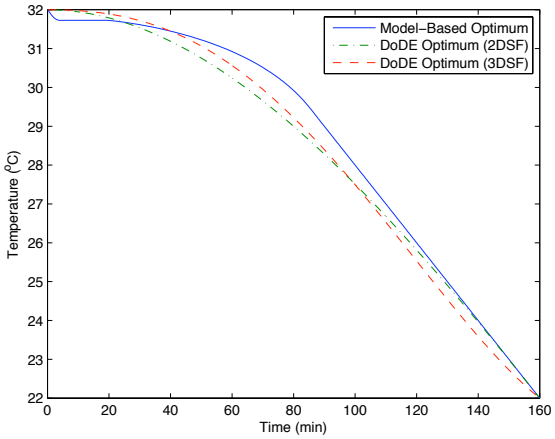

Fig. 5. Optimum temperature profiles for the optimization objective, *maximize* m_4/m_3.

these two values is close to 1 ($p-value > 0.05$) the lack of fit statistic is not significant, indicating the model is not missing any significant terms. The lack of fit statistic for each model is presented in Table 2. Each RSM has a lack of fit statistic that is nonsignificant, indicating that the form of the RSM adequately describes the data in each case.

The response surface models were optimized to find the values of the two dynamic subfactors, a_1 and a_2, that minimized m_0 and maximized m_4/m_3 within the design space (Fig. 1). The optimum values of the dynamic subfactors were used to calculate the predicted responses and 95% prediction intervals for both the m_0 and m_4/m_3 response surface models. Optimum cooling profiles were generated from (3) using the optimum dynamic subfactor values for each RSM. The crystallization model was simulated to determine the value of m_0 and m_4/m_3 using the appropriate optimized cooling trajectory. The predicted response values found using the RSM's agree with the simulated values calculated using the optimum cooling trajectories. The optimum dynamic subfactors, predicted response, and simulated response values are reported in Table 2.

Table 2. DoDE Results Summary

Response	Number of Experiments	$R^2(adj)$	$R^2(pred)$	LoF $p-value$	Optimum Values a_1	a_2	a_3	Predicted Response	Simulated Response
m_0 (2 DSF)	12	0.96	0.88	0.46	0	0.31	-	$(2.62 \pm 0.04) \times 10^6$	2.65×10^6
m_4/m_3 (2 DSF)	12	0.97	0.95	0.66	0.80	-0.20	-	$(5.79 \pm 0.07) \times 10^{-4}$	5.77×10^{-4}
m_0 (3 DSF)	21	0.95	0.91	0.76	0.08	0.45	-0.23	$(2.61 \pm 0.04) \times 10^6$	2.63×10^6
m_4/m_3 (3 DSF)	21	0.96	0.95	0.84	0.81	-0.49	-0.30	$(5.77 \pm 0.08) \times 10^{-4}$	5.78×10^{-4}

Table 3. DoDE versus Model-Based Optimum

	Objectives	
	min m_0	max m_4/m_3
Model-Based Optimum (MBO)	2.61×10^6	5.97×10^{-4}
DoDE Optimum (2 DSF)	2.65×10^6	5.77×10^{-4}
% Difference from MBO (2 DSF)	1.8%	3.4%
DoDE Optimum (3 DSF)	2.64×10^6	5.78×10^{-4}
% Difference from MBO (3 DSF)	1.1%	3.3%

Results of the optimized objectives are given in Table 3. The values reported for the DoDE optimization method were obtained by simulating the crystallization model using the optimum cooling trajectory generated from the optimum dynamic subfactor values. It is seen that the DoDE optimization is able to calculate an optimum operating trajectory that comes within 1.8% of the model-based optimum for the objective minimize m_0 and within 3.4% of the model-based optimum for the objective maximize m_4/m_3.

Three Dynamic Subfactors The two subfactor DoDE design was augmented with nine additional experimental points in order to evaluate a cooling rate profile with three dynamic subfactors (16).

$$\frac{\mathrm{d}\theta}{\mathrm{d}\tau} = -1 - a_1(2\tau - 1) - a_2(1 - 6\tau + 6\tau^2) - a_3(20\tau^3 - 30\tau^2 + 12\tau - 1) \quad (16)$$

The design space was calculated using (5)-(8) and (16) and was found to have a nonlinear bounding surface. Therefore, a D-optimal experimental design algorithm was used to augment the two dynamic subfactor experimental design and generate nine additional points in the nonlinear three dynamic subfactor design space. The dynamic factors were once again scaled to range between -1 and $+1$ and a second-order RSM was fit to the data obtained for the two response variables. The RSM was analyzed in the same manner as before. Parameter estimates and VIF values are not presented but a summary of the model and optimization results are presented in Table 2. A comparison of the DoDE optimization results for the three subfactor design versus the model-based optimization results are presented in Table 3.

A slight improvement is seen in the optimum values for the simulated responses for the three dynamic subfactor case when compared to the two dynamic subfactor case, however, based on the overlap in the predicted response data the improvement is not significant. This indicates that the addition of a third dynamic subfactor and basis function to the cooling rate profile does not improve the DoDE optimization results significantly and that a satisfactory optimum can be found with two dynamic subfactors and 12 experiments. Optimum cooling trajectories for the three dynamic subfactor case are presented in Figs. 4 and 5.

5. CONCLUSIONS

In this paper we show how the Design of Dynamic Experiments technique can be used to optimize a time-variant input profile for a batch crystallization process without the need for a first-principles model.

Using two dynamic subfactors to manipulate the cooling rate profile we were able to achieve results within a few percent of the model-based optimum. This is impressive as no first-principles model is required to perform the optimization.

This optimization methodology could be extremely useful for complex batch crystallization processes where no first-principles model exists or where the objective to be optimized cannot be expressed in terms of a first-principles model.

REFERENCES

K.L. Choong and R. Smith. Optimization of batch cooling crystallization. *Chemical Engineering Science*, 59(2):313–327, 2004.

S.H. Chung, D.L. Ma, and R.D. Braatz. Optimal seeding in batch crystallization. *Canadian Journal of Chemical Engineering*, 77 (3):590–596, 1999.

C. Georgakis. A model-free methodology for the optimization of batch processes: Design of dynamic experiments. IFAC Symposium on Advanced Control of Chemical Processes, Jul 2009.

Q. Hu, S. Rohani, and A. Jutan. Modelling and optimization of seeded batch crystallizers. *Computers and Chemical Engineering*, 29(4):911–918, 2005.

H.M. Hulburt and S. Katz. Some problems in particle technology. a statistical mechanical formulation. *Chemical Engineering Science*, 19(8):555–574, 1964.

Y.-D. Lang and L.T. Biegler. A software environment for simultaneous dynamic optimization. *Computers and Chemical Engineering*, 31(8):931–942, 2007.

Y.-D. Lang, A.M. Cervantes, and L.T. Biegler. Dynamic optimization of a batch cooling crystallization process. *Industrial and Engineering Chemistry Research*, 38(4):1469–1477, 1999.

D.C. Montgomery. *Design and Analysis of Experiments*. John Wiley & Sons, Inc., 6th edition, 2005.

R.H. Myers and D.C. Montgomery. *Response Surface Methodology: Process and Product Optimization Using Design of Experiments*. John Wiley & Sons, Inc., 1995.

Z.K. Nagy, M. Fujiwara, and R.D. Braatz. Modelling and control of combined cooling and antisolvent crystallization processes. *Journal of Process Control*, 18(9):856–864, 2008.

D. Sarkar, S. Rohani, and A. Jutan. Multi-objective optimization of seeded batch crystallization processes. *Chemical Engineering Science*, 61(16):5282–5295, 2006.

J.D. Ward, D.A. Mellichamp, and M.F. Doherty. Choosing an operating policy for seeded batch crystallization. *AIChE Journal*, 52(6):2046–2054, 2006.

J. Worlitschek and M. Mazzotti. Model-based optimization of particle size distribution in batch-cooling crystallization of paracetamol. *Crystal Growth and Design*, 4(5):891–903, 2004.

W. Xie, S. Rohani, and A. Phoenix. Dynamic modeling and operation of a seeded batch cooling crystallizer. *Chemical Engineering Communications*, 187:229–249, 2001.